# Diastereoselective Synthesis of New Rhodium-Based Amphiphilic Polyol-Cp Systems

Silvia Bordoni,*,† Paolo Natanti,† Stefano Cerini,† Riccardo Tarroni,† Magda Monari,‡ Fabio Piccinelli,‡ and Luigi Busetto†

*Dipartimento di Chimica Fisica ed Inorganica, Università di Bologna, Viale Risorgimento, 4 I-40136 Bologna, Italy, and Dipartimento di Chimica "Giacomo Ciamician", Università di Bologna, Via Selmi, 2 I-40126 Bologna, Italy*

*Received October 25, 2007*

The cyclopentadienide nucleophilic ring opening on the cyclopentene oxide affords diastereoselectively an efficient entry to a new polyalcoholic (1,2,4)-$C_5H_2[CH(CH_2)_3CHOH]_3$ propeller-like, hybrid ligand $Cp^{OOO}$. The diastereoselective rhodium complexation gives rise almost quantitatively to a new class of racemic $Cp^{OOO}Rh(L,L)$ (L,L = nbd, cod, $C_2H_4$, CO) complexes. Thermal treatment gives predominantly the air-stable $Cp^{OOO}Rh(nbd)$ *rac*-**4a** (73.5%), having $S_P$ planar chirality, as determined by X-ray diffraction studies. It has also been possible to isolate its stable atropisomer *rac*-**4c** (20.5%), while the minor kinetic isomer *rac*-**4b**, showing opposite planar chirality (∼10%), has been identified by NOESY NMR experiments. The high solubility in water and benzene, evidencing the amphiphilic character, has been measured by the *n*-octanol/water partition coefficient. The intermolecular H-binding, due to the hydroxy groups, plays a crucial role in selecting the rhodium coordination in the reaction mixture, whereas in the solid, it determines the supramolecular organization. DFT calculations in vacuo are in agreement with the spectroscopically identified structures.

## Introduction

Appending hydroxyl side chain to ligands as in $R_2P(CH_2)_nOH$ ($n$ = 2–4) constitutes a well-known strategy[1] to transfer hydrophilic features to coordinated metal complexes. In this context, the cyclopentadienyl ring can be considered as ubiquitous as phosphine ligands to provide a general access to fine control of the steric and electronic properties in new single-site catalysts, which may permit a more benign chemistry, compelled by the urgent demand of reducing environmental impacts.[1d] The chosen synthetic route to multihydroxy Cp (Cp = $\eta^5$-$C_5H_5$) ligands adopts the well-attested and convenient epoxide ring opening[2] of cyclopentene oxide $[CH(CH_2)_3CH]O$ by sodium cyclopentadienide (NaCp), followed by prompt proton O-migration. Despite the increased kinetic stability imparted to the aromatic ring by the donor-tether substituents, the class of multifunctionalized Cp ligands is still underrepresented, primarily for stereoelectronic reasons connected to synthetic procedures.[3]

## Results and Discussion

The tandem alkylation/H-transfer reaction affords a racemic mixture of 1-(2-hydroxycyclopentyl)cyclopenta-2,4-dien-1-ide, $Na[C_5H_4(CH(CH_2)_3CHOH)]$ (**1**, 2′*R/S*, $NaCp^O$), in good yield (70–80%) and under moderate conditions, as outlined in Scheme 1, path *a*.[4] The one-pot 2-fold addition (*b*′), or alternatively two sequential additions of epoxide (*a*+*b*), generates exclusively the 1,3-bis(2-hydroxycyclopentyl)cyclopenta-2,4-dien-1-ide, $Na[C_5H_3(CH(CH_2)_3CHOH)_2]$ (**2**, $NaCp^{OO}$), derivative, which is a mixture of three isomers: one couple of enantiomers 1,3-(2′*R*,2″*R*) **2a** and (2′*S*,2″*S*) **2a**′ and one *meso* form 1,3-(2′*R*,2″*S*) **2b**. The incorporation of a third oxirane moiety (*b*) leads to the formation of 1,2,4-tris(2-hydroxycyclopentyl)cyclopenta-2,4-dien-1-ide, $Na[C_5H_2(CH(CH_2)_3CHOH)_3]$ (*rac*-**3**, $NaCp^{OOO}$), as a light brown, powdered solid. The reaction goes to completion by addition of a further epoxide equivalent to the supernatant or by a one-step 5-fold addition (*b*″).

The neutralization with water of *rac*-**1** or *rac*-**2** forms an equimolar mixture of the corresponding tautomers $Cp^OH$ and $Cp^{OO}H$. Analogously, water quenching of *rac*-**3** gives a pale orange, powdered solid, mostly composed by a racemic couple of $Cp^{OOO}H$ diastereomers identified by NMR as 2′,2″,2‴-(cyclopenta-1,3-diene-1,2,4triyl)tricyclopentanol species, *rac*-

* Corresponding author. E-mail: silvia.bordoni@unibo.it.
† Dipartimento di Chimica Fisica ed Inorganica.
‡ Dipartimento di Chimica "Giacomo Ciamician".

(1) (a) Hermann, W. *Aqueous-Phase Organometallic Catalysis*; VCH: Weinheim, 2004; p 187. (b) Jensen, V. R.; Jolly, P. W.; Thiel, W.; Weber, J. C. *Organometallics* **2001**, *20*, 2234–2245. (c) Mebi, C. A.; Nair, R. P.; Frost, B. J. *Organometallics* **2007**, *26*, 429–438. (d) Bolano, S.; Gonsalvi, L.; Zanobini, F.; Vizza, F.; Bertolasi, V.; Romerosa, A.; Peruzzini, M. *J. Mol. Catal. A: Chem.* **2004**, *224*, 61–70.

(2) (a) Howell F. H.; Taylor D. A. H. *J. Chem. Soc.* **1957**, 3011. (b) Cuvigny, T.; Normant, H. *Bull. Soc. Chem. Fr.* **1964**, *5*, 2000. (c) Hauck F. P.; Sunden J. E.; Reid J. (E.R. Squibb & Sons, Inc.) Patent Appl. N. US1978000928483, 1979. (d) Panarello, A. P.; Vassylyev, O.; Khinast, J. G. *Synlett.* **2005**, *5*, 797–800. (e) Trifonov, A.; Fedorova, E. A.; Kirillov, E. N.; Nefedov, S. E.; Ermenko, I. L.; Kurskii, Yu. A.; Shavyrin, A. S.; Bochkareva, M. N. *Russ. Chem. Bull. Int. Ed.* **2002**, *51*, 684. (f) Siemeling, U. *Chem. Rev.* **2000**, *100*, 1495–1526.

(3) (a) Deck, P. A. *Coord. Chem. Rev.* **2006**, *250*, 1032–1055. (b) Steurer, M.; Tiedl, K.; Wang, Y.; Weissensteiner, W. *Chem. Commun.* **2005**, 4929–4931. (c) Costa, M.; Dalcanale, E.; Dias, F. S.; Graiff, C.; Tiripicchio, A.; Bigliardi, L. *J. Organomet. Chem.* **2001**, *619*, 179–193. (d) Davenport, A. J.; Davies, D. L.; Facwett, J.; Russell, D. R. *J. Organomet. Chem.* **2006**, *691*, 2221–2227. (e) Pool, J. A.; Chirik, P. J. *Can. J. Chem.* **2005**, *83*, 286–295. (f) Uno, M.; Ando, K.; Komatsuzaki, N.; Takahashi, S. *J. Chem. Soc., Chem. Commun.* **1992**, 964–965.

(4) (a) Brookings, D. C.; Harrison, S. A.; Whitby, R. J.; Crombie, B.; Jones, R. V. H. *Organometallics* **2001**, *20*, 4574–4583. (b) Trifonov, A. A.; Ferri, F.; Collin, J. *J. Organomet. Chem.* **1999**, *582*, 211–217. (c) Rieger, B. *J. Organomet. Chem.* **1991**, *420*, C17–C20. (d) Ohta, H.; Kobori, T.; Fujisawa, T. *J. Org. Chem.* **1977**, *42*, 1231–1235.

10.1021/om701073h CCC: $40.75 © 2008 American Chemical Society
Publication on Web 02/09/2008

**Scheme 1. Synthesis of Multihydroxy Ligands and the Corresponding Rh Complexes**[a]

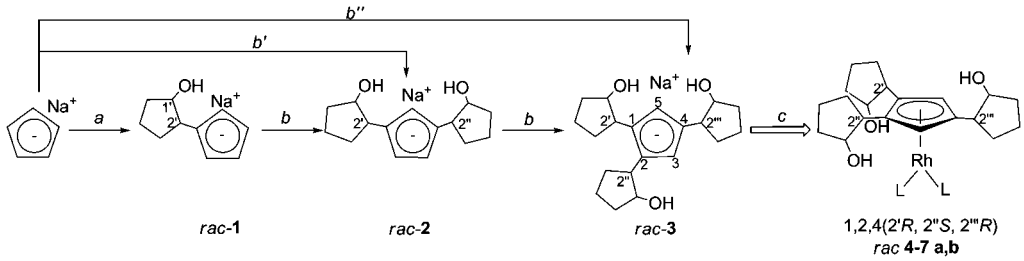


[a] Reagents and reaction conditions: epox = $[CH(CH_2)_3CH]O$; $[Rh(L,L)Cl]_2$ [L,L: nbd = $C_7H_8$, cod = $C_8H_{12}$, $C_2H_4$, CO], DME = $[CH_3O(C_2H_4)OCH_3]$. (*a*) 1 epox, THF, RT, 12 h; (*b*) 1 epox, DME, rfx, 8 h; (*b′*) 2 epox, DME, rfx, 10 h; (*b″*) 5 epox, DME, rfx, 5 h; (*c*) $[Rh(L,L)Cl]_2$ in THF, rfx, 12 h; or alternatively RT, THF, 37 h. For clarity reasons, in the cycloalkyl linker only one descriptor (C2′) of the chirotopic centers (C1′ and C2′) is explicitly shown.

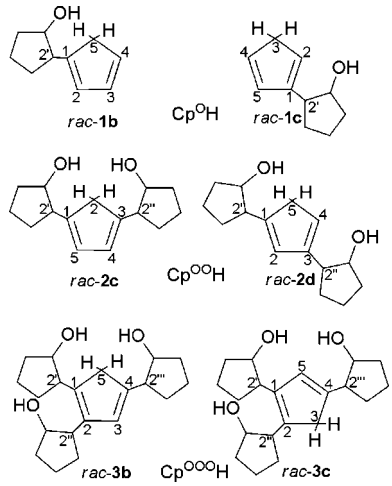


**Figure 1.** Neutralized ligands: $Cp^{O}H$ [*rac*-**1b**: 2′-(cyclopenta-1,3-dienyl)cyclopentanol, *rac*-**1c**: 2′-(cyclopenta-1,4-dienyl)cyclopentanol]; $Cp^{OO}H$ [*rac*-**2c**: 2′,2″-(cyclopenta-3,5-diene-1,3dyil)dicyclopentanol, *rac*-**2d**: 2′,2″-(cyclopenta-1,3-diene-1,3dyil)dicyclopentanol]; $Cp^{OOO}H$ *rac*-**3b**: 2′,2″, 2‴-(cyclopenta 1,3-diene-1,2,4-triyl)tricyclopentanol; *rac*-**3c**: 2′,2″,2‴-(cyclopenta-1,4-diene-1,2,4-triyl)tricyclopentanol. The peculiar (2′,2″,2‴) stereogenic methyne centers are evidenced.

**3b**, and 2′,2″,2‴-(cyclopenta-1,4-diene-1,2,4triyl)tricyclopentanol species, *rac*-**3c** (see Figure 1).

In spite of the increased complexity of the related mixture, the NMR spectroscopic features of the neutral compound unambiguously indicate the nature of the parent anions (see Scheme 1). As a consequence of the cyclopentanol crowding, attack at the C-2 atom of the $NaCp^{OO}$ **2** is hampered and only C-4 and C-5 carbons are active to further epoxide additions (Chart 1). The *cis* geometry of the cyclopentene oxide forces the methyne chirotopic atoms (C1′) and (C2′) to exhibit opposite stereocenter (*R*,*S*) configurations. Therefore, the antiperiplanar epoxide opening by the *meso*-form **2b** can generate both couples of enantiomers (**3a**, **3a′**) and the *rac*-**3a‴**. Instead, in the $C_2$-symmetric enantiomeric pair (**2a**, **2a′**), the homotopic C4 and C5 carbon atoms give rise to *rac*-**3a″** forms (Chart 1). Probably because of steric congestion, the third incorporated cyclopentanol prefers to assume the opposite chiral configuration of the adjacent substituent, giving $Cp^{OOO}$ almost diastereoselectively as *rac*-**3a** in 94% yield, while *rac*-**3a″** and *rac*-**3a‴** are present only as traces (ca. 3% each, evaluated from $^1$H NMR spectra).

The $\pi$-coordination of the trisubstituted *rac*-**3** forms an isomeric mixture almost quantitatively. The NMR spectra of the crude product $[C_5H_2(CH(CH_2)_3CHOH)_3Rh(L,L)$; L,L = nbd **4**, cod **5**, $C_2H_4$ **6**, CO **7**] obtained by thermal treatment (Scheme 1, path *c*) show a large prevalence (87–96% yield) of two distinct diastereomers, exhibiting the same diastereomeric ratio (~3:1) independently of L,L coligands, as outlined in Table 1 for entries **4**−**7**.

The synthesis of **4**, run either under high- or room-temperature reaction conditions, accomplishes almost complete conversion (94%). Separation of the crude **4** (L,L = nbd) by silica column chromatography gives rise to two distinct dark yellow fractions, whose NMR spectra exhibit similar pattern, whereas their ESI-MS spectra define a unique molecular ion. The first eluted fraction is always predominant, while the nature of the second minor fraction is strongly dependent on the reaction conditions. The former exhibits unexpected air stability in both the solid or THF solution, as monitored by NMR spectroscopy for prolonged times. As a proof of their amphiphilic character, the two dark yellow species reveal a marked solubility in both water (15.9 g $L^{-1}$) and benzene (8.6 g $L^{-1}$).[5c] In principle, the two diastereomers should correspond to distinct approaches of the Rh(nbd) moiety toward the opposite sides of *rac*-**3**, generating *rac*-**4a** and *rac*-**4b**, respectively, as shown in Scheme 2.

The metal coordination on the opposite faces of **3a** would form a couple of diastereomers, differing in planar chirality (**4a**, **4b**). Surprisingly, the thermal treatment gives rise exclusively to a single diastereomer in two distinct atropisomers: the thermodynamically stable **4a** (73.5%) and its rotameric form **4c** (20.5%), generated by the inversion of the alcoholic side arms (Scheme 3).[6]

The reaction at room temperature affords as a minor compound (~10%) the expected *rac*-**4b** ($R_P$) in an equimolar mixture with *rac*-**4c**. The analysis of the $^1$H NMR spectra in the 2–3 ppm interval (Figure 2), obtained by the two fractions under different reaction conditions, constitutes a distinctive probe for determining the relative structures. In fact, while the Cp methyne moieties are all equivalent in **4a**, in the case of *rac*-**4b**, only the signals related to C2′*H*Cp and C2″*H*Cp (2.49 ppm) are isochronous; *rac*-**4c** exhibits distinct multiplets at 2.83, 2.74, and 2.33 ppm, respectively.

The nature of the minor compound *rac*-**4c** has been investigated by monitoring ($^1$H NMR at 253 K in THF-$d_8$ solution) the complete transformation of the latter into the thermodynamically stable *rac*-**4a**. Several tests of stability in different solvents have been performed. After 480 h, the $^1$H NMR spectrum of *rac*-**4c** ($^1$H NMR, $\delta$ 4.99, 4.85) shows two additional signals ($\delta$ 4.91, 4.78) of comparable intensity and coincident with those

(5) (a) Leo, A. *Handbook of Property Estimation Methods for Chemicals: Environmental and Health Sciences*; CRC Press, 2000; Chapter 5. (b) Danielsson, L. G.; Zhang, Y. H. *Trends Anal. Chem.* **1996**, *15* (4), 188–196. (c) Chen, Z.; Weber, S. G. *Anal. Chem.* **2007**, *79*, 1043–1049.

(6) Williams, P.; Giralt, E. *Chem. Soc. Rev.* **2001**, *30*, 145–157.

**Chart 1. Central Chirality for the Peculiar Stereogenic Centers (2′,2″,2‴) in the Propeller-like $Cp^{OOO}$ Is Depicted with Filled/Empty Descriptors[a]**

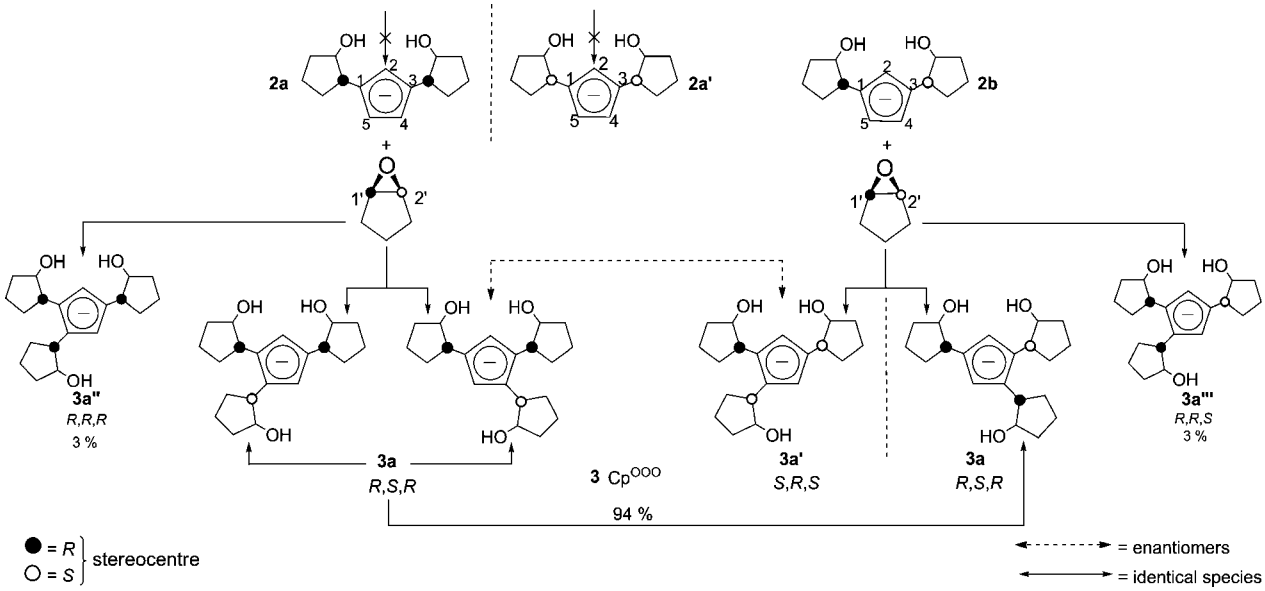


[a] Chiral descriptors (*R*,*S*) are assigned only to the carbons undergoing nucleophilic attack from Cp. Starting from **2** $Cp^{OO}$, the reaction pathway is described only for **2a** (*R*,*R*) and for the *meso*-**2b** form. Nevertheless, the reaction provides the formation of the other two **3a′** molecules from the enantiomeric form **2a′** (*S*,*S*). Traces (3%) of homochiral *rac*-**3a″** and *rac*-**3a‴** are also obtained.

**Table 1. Synthesis of Ligands and Rhodium Complexes**

| entry | Cp[a] | L,L | yield[b] [%] | d.r. I:II[c] |
|---|---|---|---|---|
| 1 | $Cp^{O}$ | | 70 | |
| 2 | $Cp^{OO}$ | | 75 | 1:1 |
| 3 | $Cp^{OOO}$ | | 94 | |
| 4 | $Cp^{OOO}$ | nbd | 94 | 3.0:1 |
| 5 | $Cp^{OOO}$ | cod | 93 | 2.9:1 |
| 6 | $Cp^{OOO}$ | $C_2H_4$ | 87 | 2.9:1 |
| 7 | $Cp^{OOO}$ | CO | 96 | 2.9:1 |

[a] $Cp^{O}$ = $[C_5H_4(CH(CH_2)_3CHOH)]$, $Cp^{OO}$ = $[C_5H_3(CH(CH_2)_3CHOH)_2]$, $Cp^{OOO}$ = $[C_5H_2(CH(CH_2)_3CHOH)_3]$. [b] Yields are derived by weighting after purification the isolated air-sensitive $NaCp^{O}$, $NaCp^{OO}$, and $NaCp^{OOO}$. [c] Diastereomeric ratio for **4**−**7** is determined by the weight of the crystallized compounds; in the case of entry 2 by the $^1$H NMR ratio of the isomeric mixture.

**Scheme 2. In the More Abundant Isomer *rac*-4a, the Rh(nbd) Fragment Coordinates the $Cp^{OOO}$ Ligand from the More Hydrophilic Face of 3a (2′*R*, 2″*S*, 2‴*R*)**

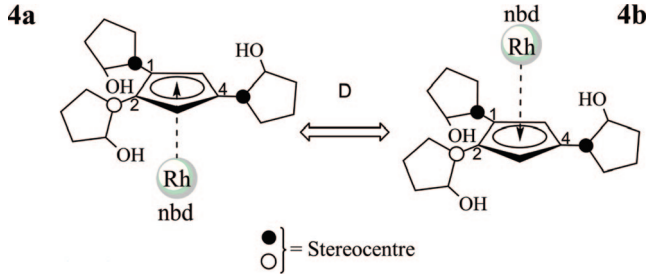


detected for *rac*-**4a**. A faster (5 h) analogous behavior is observed in refluxing MeOH-$d_4$. No trace of Rh decomposition or release of neutral ligand has been detected under the conditions utilized, although decomplexation of the penthapto $Cp^{OOO}Rh$ system cannot be dismissed a priori. On the other hand, **4a** remains unchanged in toluene (115 °C, 9 h), and only traces of $Cp^{OOO}H$ (∼3%) have been detected. Finally, pure *rac*-**4c** converts completely into *rac*-**4a** by refluxing for 2 h in DMSO. In summary, thermal transformation of the minor isomer is promoted only by high-polar and -donor solvents, responsible

**Scheme 3. Central Chirality for the Peculiar Stereogenic Centers (2′,2″,2‴) in the $Cp^{OOO}$ Is Depicted with Filled (●=*R*)/Empty (○=*S*) Descriptors[a]**

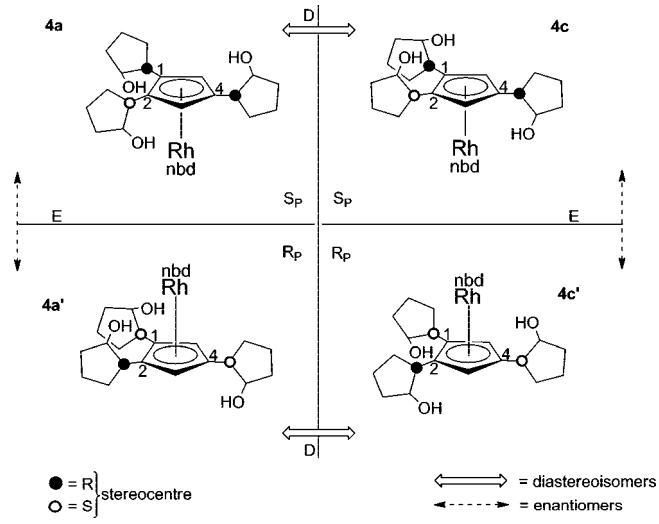


[a] **4a** and **4c**, both showing $S_P$ planar chirality, differ only in the *endo* or *exo* position of the two vicinal hydroxyl groups, respectively.

for altering significantly the torsion angles ($\varphi_1$ and $\varphi_2$). These findings confirm the identification of **4c** as a stable rotameric form of **4a**. In fact, side-arm rotation produces the distinct atropisomer *rac*-**4c**, retaining the $S_P$ planar chiral configuration. Preliminary gas-phase ab initio calculations on anionic ligand *rac*-**3** $[Cp^{OOO}]^-$, predicting a fairly low-energy rotational barrier (∼7 kcal mol$^{-1}$) for the vicinal 1,2 substituents, support this speculation. In addition, NOESY experiments performed on *rac*-**4a** confirm a neat preference (d.r. 3:1) for the Rh(nbd) fragment to anchor at the most hydrophilic face, suggesting the retention in solution of the structure determined by both X-ray and density functional studies. Indeed, irradiation of C3*H*Cp and C5*H*Cp signals causes respectively the maximum enhancement effect

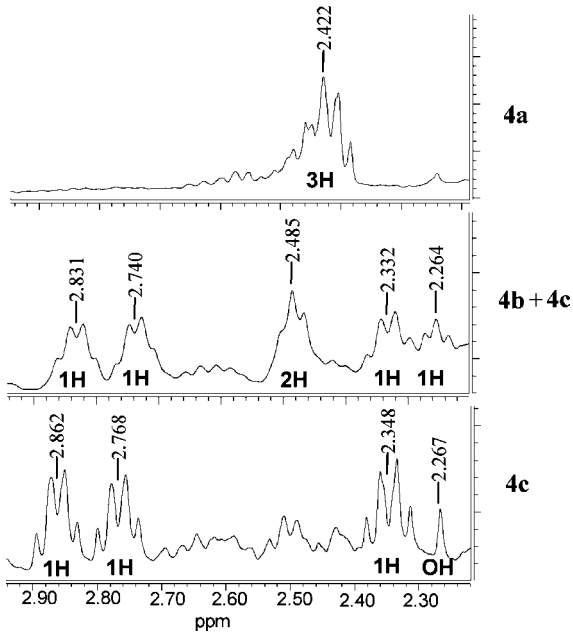


**Figure 2.** $^1$H NMR portion in the 2–3 ppm range: the C2*H*Cp signals are indicative for designing the stereochemistry of the **4a**, **4b**, and **4c** Rh isomers.

on the $\delta$ 3.82 (C1″*H*OH; 65%) and 3.76 (C1′*H*OH; 100%) resonances, belonging to methyne moieties of substituents 1 and 2 (see Figure 3). The same experiment, performed on the minor species influences the outer methyne moieties C2′*H*Cp ($\delta$ 2.86; 73%) and C2″*H*Cp ($\delta$ 2.34; 77%) and gives rise to marked enhancement (100%) of nbd olefin signals ($\delta$ 3.11), disclosing for the two vicinal cycloalkyl moieties a preferred closer position, which bears the hydroxyl groups reciprocally face up. These observations indicate *rac*-**4c** as the structure attributed to the minor compound. Conversely in *rac*-**4b**, the signal at $\delta$ 3.94 of substituent 4 (C1‴*H*OH) would be the only one affected by saturation of the C3*H*Cp. Furthermore, the related 1,2 vicinal cyclopentanol groups would be oriented reciprocally apart, forcing the C2*H*Cp moieties to assume reciprocally inner-facing position. The vicinal hydroxyl groups of *rac*-**4a** and *rac*-**4c**, which respectively are *endo* or *exo* to the metal coordination, both exhibit *trans* orientation concerning substituent 4 (see NOE experiments in the Supporting Information, tables, and Figures S9 and S10).

As a proof of the similar orientation of hydroxyl groups, we were unable to separate by chromatography *rac*-**4b** and *rac*-**4c**, whereas the first fraction, corresponding to *rac*-**4a**, has been crystallized and structurally characterized by X-ray diffraction studies. In the crystal, both enantiomers **4a** (Figure 4) and **4a′** are present. For the enantiomer **4a** the stereogenic configurations are $S_P$[1-(2′*R*), 2-(2″*S*), 4-(2‴*R*)]Cp$^{OOO}$Rh(nbd) and $R_P$[1-(2′*S*), 2-(2″*R*), 4-(2‴*S*)]Cp$^{OOO}$Rh(nbd) for **4a′**. Under addition of a chiral solvating agent to the crude *rac*-**4a**, the corresponding $^1$H NMR spectra display equal enantiomeric abundance, reflecting the same racemic distribution in solution.[7]

To define the rank of the chirotopic atoms sequence and therefore inferring planar chirality, in the presence of "reflection-variant" groups, the CIP priority rules[8] suggest seeking any geometrical differences. The Cp$^{OOO}$ is a propeller-like ligand, which exhibits a counterclockwise helicity. The two enantiomorphic vicinal substituents 1 and 2, being related by a $C_2$ local symmetry, are opposite in the chiral definition and the application of the sequence rules does not lead to a definite description for the planar chiral determination. In this context, as distinctive geometrical element for defining the (1,2,4)-anticlockwise sequence of the **4a** helical conformation, we propose instead the analysis of the torsional dihedral angles $\varphi_1$, $\varphi_2$, and $\varphi_4$ (Figure 5), spanned between the cyclopentadienide plane and the cyclopentanol substituents [e.g., $\varphi_1'$ (C5C1C2′C1′)].

Significantly, the designation of the helicity of **4a** would depend on the dihedral angles of vicinal 1- and 2-hydroxy blades ($\varphi_1$, $\varphi_2$). Although in the crystal structure these angles show values consistently different from the theoretical ones (see Figure 5), the $S_P$ helicity,[9] inferred by both X-ray diffraction studies and in vacuo calculations, results in agreement with helical $\Lambda$ description. To clarify such a peculiar behavior, ab initio density functional investigations have been carried out on *rac*-**4a** and *rac*-**4b** and on two higher energy conformers, named *rac*-**4c** and *rac*-**4d**, respectively.

The DFT calculations lead to equilibrium structures with very close energies. Taking the *rac*-**4a** structures as reference, the energies of *rac*-**4b** are calculated to be at $-3.1$ kcal mol$^{-1}$, while *rac*-**4c** and *rac*-**4d** are at $+5.7$ and $+5.8$ kcal mol$^{-1}$, respectively (for the corresponding structures, see Figure 6). The energy value for *rac*-**4b** is at odds with respect to the experimental finding, which points to *rac*-**4a** as the thermodynamically favored species. However, the neglect of solvent effects in the computations may be invoked to explain the found discrepancy. Indeed, the lack of solute–solvent intermolecular interaction favors the formation of a tight intramolecular hydrogen bond (1.93 Å) between the hydroxy groups of 1,2 cyclopentanol substituents in *rac*-**4b**, leading to further stabilization compared to *rac*-**4a**. Although in principle *rac*-**4d**, as a rotamer of *rac*-**4b**, should be present, surprisingly no occurrence has been seen in the NMR spectra of the studied mixtures.

As mentioned above, the **4a** and **4a′** enantiomers crystallize together. In the crystal packing, the intermolecular hydrogen bonds generate corrugated infinite chains along the *a* axis, consisting of two different types of alternating fused 18-membered rings and 24-membered macrocycles. In the 18-membered rings (Figure 7), the dimers arising by the two molecules **4a** and **4a′** are held together by two symmetry-related hydrogen bonds, involving the hydroxyl groups O1−H1 and O2−H2, located on the same side of the Cp occupied by the Rh(nbd) unit. The larger 24-membered macrocycles share these two intermolecular H-bonds of the former rings, and each oxygen atom of the O1−H1 groups is further involved in two extra H-bonds with the O4−H4. One chloroform molecule for each Rh complex is stabilized by a further hydrogen interaction (H4−O4···H) group. The supramolecular network generated by H-bonds is responsible for the self-arranging of the racemic species in the crystal packing.

(7) Pirkle, W. H. *J. Am. Chem. Soc.* **1966**, *88*, 1937.

(8) (a) Atributed by applying the CIP sequence rule 5: p 575: *R* > *S* subrule of Rule 4 "*r* precedes *s*" Prelog, V.; Helmchen, G. *Angew. Chem. Int. Ed.* **1982**, *21*, 567–584. (b) Sloan, T. *Top. Stereochem.* **1981**, *12*, 139 (p. 10) .

(9) (a) The stereodescriptors related to the planar chirality are used according to: Schlögl, K. *Top. Stereochem.* **1967**, *1*, 39. (b) Baker, R. W.; Wallace, B. J. *Chem. Commun.* **1999**, 1405–1406. (c) Koelle, U.; Bücken, K.; Englert, U. *Organometallics* **1996**, *15*, 1376–1383. (d) Paley, R. S. *Chem. Rev* **2002**, *102*, 1493–1523. (e) Curnow, O. J.; Ferm, G. M. *Organometallics* **2002**, *21*, 2827–2829. (f) Lee, J. H.; Son, S. U.; Chung, Y. K. *Tetrahedron: Asymmetry* **2003**, *14*, 2109–2113. (g) Gutnov, A.; Drexler, H. J.; Spannenberg, A.; Oehme, G.; Heller, B. *Organometallics* **2004**, *23*, 1002–1009.

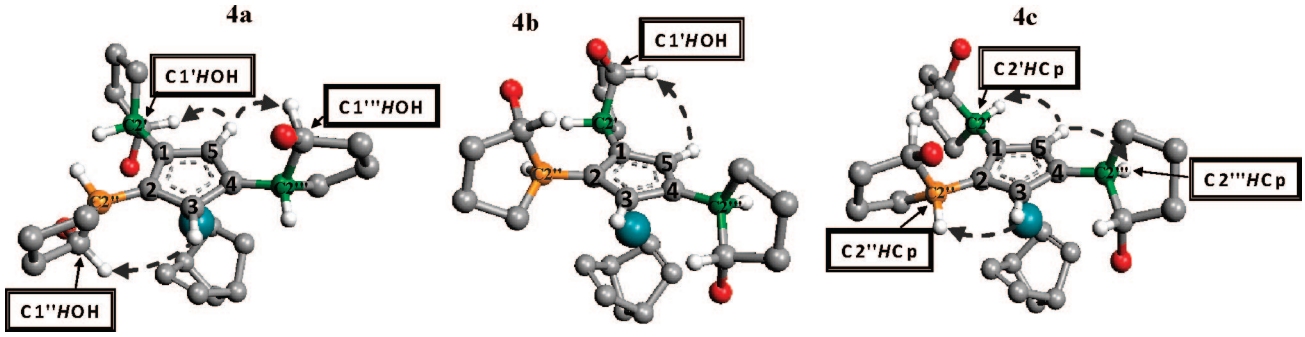


**Figure 3.** Labeling scheme for **4a**,**b**,**c** $Cp^{OOO}Rh(nbd)$ and main NOE interactions shown by curved arrows.

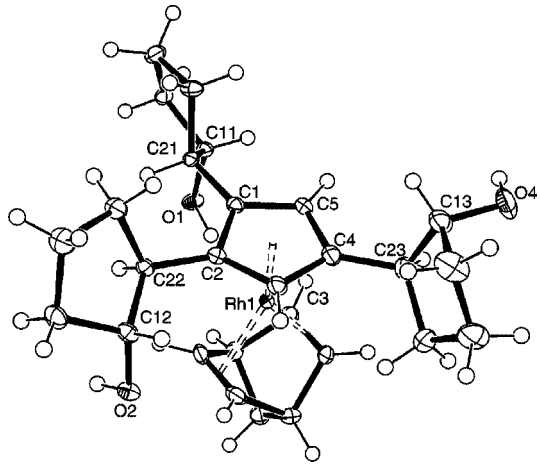


**Figure 4.** ORTEP drawing of the dominant (73.5%) isomer *rac*-**4a** (only one enantiomer is shown, thermal ellipsoids drawn at 50% probability level). Planar chirality: $S_P$. Configurations of relevant stereogenic centers: C(21)(*R*); C(22)(*S*); C(23)(*R*) (correspondences to labels of Scheme 1: C21′C2′, C22′C2″, C23′C2‴).

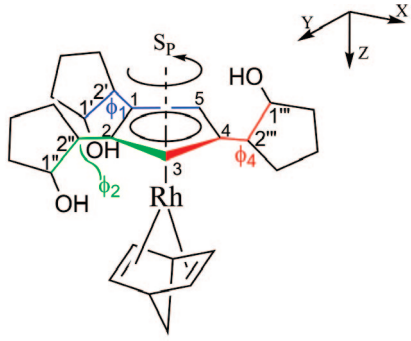


| | X-Ray | | | DFT | | |
|---|---|---|---|---|---|---|
| | $\phi_1$ | $\phi_2$ | $\phi_4$ | $\phi_1$ | $\phi_2$ | $\phi_4$ |
| *rac*-**4a** | +18.2 | -46.9 | -86.2 | +60.5 | -92.6 | -99.4 |
| *rac*-**4b** | - | - | - | +86.7 | -64.0 | -143.6 |
| *rac*-**4c** | - | - | - | -61.2 | +85.6 | +31.1 |

Substituent 1 = C5C1C2′C1′
Substituent 2 = C3C2C2″C1″
Substituent 4 = C3C4C2‴C1‴

**Figure 5.** Computed and X-ray diffraction determined $\varphi$ torsion angles (deg) in *rac*-**4a**. DFT calculations predict the geometry for the minimum energy conformations in vacuo of **4a**, **4b**, and **4c** (see text).

As suggested by the X-ray structure, strong intermolecular O−H···O hydrogen-bonding interactions, more than steric reasons, may promote diastereoselective coordination. Although

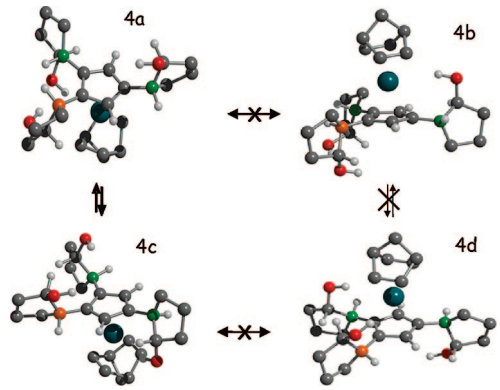


**Figure 6.** DFT minimum energy structures for the $Cp^{OOO}Rh(nbd)$ species **4a**, **4b**, **4c**, and **4d**. Only the peculiar methyne chirotopic atoms (C1*H*OH and C2*H*Cp) are depicted. C2*H*Cp, which are responsible for the chiral definition, are colored either green (*R*) or orange (*S*).

calculations designated the isomer *rac*-**4b** as the thermodynamically preferred, the H-binding interactions promote the formation of *rac*-**4a**.

To examine this point in solution, we have monitored the $\delta$ trend relative to the OH groups by $^1$H NMR VT experiments. In agreement with peptide, alcohol, and carbohydrate behavior,[10] the strongly downfield-shifted hydroxy NMR signals (*rac*-**4a**: $\delta$ 3.2–5.5 in $CDCl_3$; 5.7–6.6 in Py-$d_5$) and the high values of the temperature coefficients ($\Delta\delta/\Delta T \approx -11$ ppb/K) (Table 2 and Figure 8) indicate the occurrence of strong intermolecular OH···O hydrogen-bonding interactions. In accord with the DFT calculations, which suggest a tight intramolecular H-bond interaction with the vicinal hydroxyl groups, the OH moiety of substituent 2 interestingly shows the scarcest solvent dependence ($-\Delta\delta/\Delta T = 5.3$ ppb/K) even in progressively diluted solutions ($CDCl_3$, 0.18 M, 11 mM, 5 mM). It is worth noting that the hydroxyl moieties of *rac*-**4c** exhibit narrower temperature coefficient trends than the relative *rac*-**4a**, in either coordinating (Py-$d_5$) or noncoordinating solvents ($CDCl_3$). This finding constitutes further support for its structure in solution, as easier solvating interactions are in line with the Rh(nbd) coordination opposite the cyclopentanol side arms.

The evaluation of C1*HOH* torsional angles ($\theta$, see inset of Table 3) by the $^3J$ NMR coupling constants[11] of the distinct

(10) (a) Belvisi, L.; Gennari, C.; Mielgo, A.; Potenza, D.; Scolastico, C. *Eur. J. Org. Chem.* **1999**, *5*, 389–400. (b) Lomas, J. S. *J. Chem. Soc., Perkin Trans. 2* **2001**, 754–757. (c) Lomas, J. S.; Adenier, A.; Cordier, C.; Lacroix, J. C. *J. Chem. Soc., Perkin Trans. 2* **1998**, 2647–1652. (d) Bernet, B.; Vasella, A. *Helv. Chim. Acta* **2000**, *83*, 995–1021.

(11) Fraser, R. I.; Kaufman, M.; Morand, P.; Govil, G. *Can. J. Chem.* **1969**, *47*, 403–409.

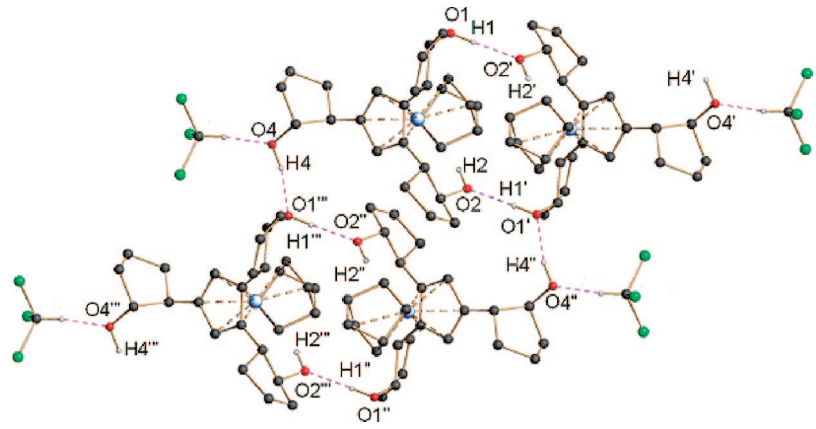


**Figure 7.** Structural motif present in the crystal packing: alternation of fused 18-membered and 24-membered macrocycles built by intermolecular H-bonds. O1−H1···O2′, 0.94(2), 1.91(2), 2.856(3) Å, 177(3)°; O4−H4···O1‴ 0.95(2), 1.84(2), 2.786(3) Å, 165(4)°. Symmetry code (I): 1−*x*, −*y*, −*z*; (II) –*x*, −*y*, −*z*; (III) –1+*x*, *y*, *z*.

**Table 2. NMR High-Temperature Coefficients $-\Delta\delta$(OH)/$\Delta T$ (ppb/°C) of the Hydroxyl Groups of *rac*-4a and *rac*-4c at 298–328 K**

| solvent | OH | **4a**[a] ($R^2$) | **4c**[b] ($R^2$) | cyclopentanol ($R^2$) |
|---|---|---|---|---|
| $CDCl_3$ | 1 | 10.6 (1.000) | 13.1 (0.894) | 3.5 (0.998) |
| | 2 | 5.3 (1.000) | 14.4 (0.933) | |
| | 4 | 10.3 (0.999) | 14.4 (0.933) | |
| Py-$d_5$ | 1 | 16.4 (0.999) | 11.2 (0.992) | 15.6 (0.999) |
| | 2 | 12.3 (0.999) | 16.7 (0.999) | |
| | 4 | 12.1 (0.999) | 15.1 (0.997) | |

[a] $CDCl_3$, 0.18 M; Py-$d_5$, 0.09 M. [b] $CDCl_3$, 18 mM; Py-$d_5$, 7.0 mM.

hydroxy signals suggests values of dihedral angles consistent with those obtained in the solid and from DFT (Table 3). The similar values found in solution and by calculations may indicate close minimum energy conformations. On the other hand in the solid, the intermolecular H-bonds significantly alter the vicinal $\theta_1$ and $\theta_1$. The analysis of the crystal packing of **4** shows indeed that the 1,2 hydroxyl groups of **4a** interact reciprocally with the enantiomeric counterpart **4a′** and with the OH belonging to substituent 4. Thus, even in solution the intermolecular H-binding network prevails on the stabilizing intramolecular bond shown by the vicinal side-arm O−H···O interaction under vacuum (1.926 Å).

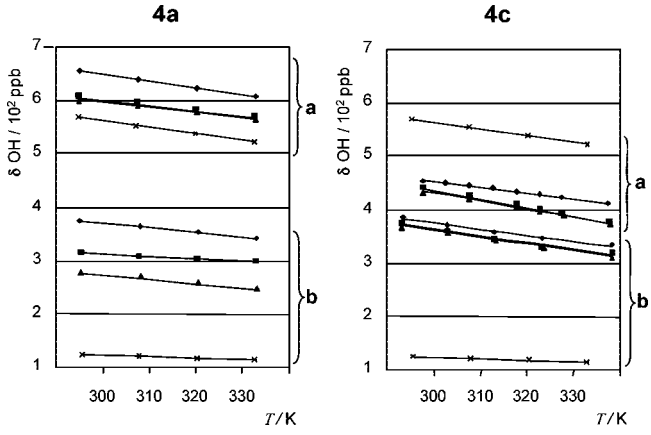


**Figure 8.** VT $^1$H NMR trend for the hydroxyl groups of *rac*-**4a** and *rac*-**4c** in the 213–333 K temperature interval (a: $CDCl_3$; b: Py-$d_5$): [♦ $\Delta\delta$ OH(1); ■ $\Delta\delta$ OH(2); ▲ $\Delta\delta$ OH(4); × $\Delta\delta$ OH cyclopentanol as reference].

**Table 3. Comparison of the Absolute Values of C1*HOH* Dihedral Angles $\theta_1$, $\theta_2$, and $\theta_4$, Corresponding to (1,2,4) Substituents Obtained in the Solid State, from Gas-Phase DFT, and in Solution by Using the Pseudo-Karplus Relationship: $^3J$(C′H,OH) = 10.4 cos$^2$ $\theta$ – 1.5 cos $\theta$ + 0.2**

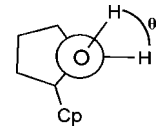


| **4a** | $CDCl_3$ | X-ray | calcd |
|---|---|---|---|
| $\theta_1$ | 53.4 | 179.1 | 56.9 |
| $\theta_2$ | 57.5 | 74.5 | 67.6 |
| $\theta_4$ | 61.9 | 59.5 | 60.7 |

## Conclusion

A diastereoselective entry to a new class of polyol-hybrid cyclopentadienyl ligands and the corresponding *rac*-(**1**,**2**,**4**)-Cp$^{OOO}$Rh(nbd) complexes have been efficiently accomplished. The high solubility in both water and benzene, together with the elevated octanol/water partition coefficient, evidencing their marked amphiphilic features, makes them potential single-site precatalysts for homogeneous or multiphase applications.[12] The spatial arrangements found in solution by NOESY NMR experiments are mostly in agreement with the DFT-calculated structures. However, in contrast with the calculated minimum energies, the hydroxyl group H-bonds seem to prevail over the steric requirements. The reaction affords predominantly the species *rac*-**4a** as the thermodynamically stable one. The X-ray structure evidences a remarkable intermolecular H-bonding interaction. Although the calculations in the absence of medium indicate as predominant the *rac*-**4b** isomer, showing opposite planar chirality ($R_P$), it has been obtained only in limited amount (ca. 10%). The rotation of the hydroxyl side arms gives rise to the stable atropisomer *rac*-**4c**, exhibiting for the Rh fragment opposite coordination.

Since the two Cp$^{OOO}$ diastereofaces show similar steric hindrance, the found unbalanced amount between the two diastereomers might be a consequence of the diastereoselective preference of the metal to coordinate the more hydrophilic Cp$^{OOO}$ side.

(12) (a) Paetzold, E.; Jovel, I.; Oehme, G. *J. Mol. Catal. A: Chem.* **2004**, *214* (2), 241–247. (b) Frost, B. J.; Mebi, A. C. *Organometallics* **2004**, *23*, 5317–5323.

## Experimental Section

**General Remarks.** All the manipulations were carried out under argon atmosphere and by using standard Schlenk techniques with anhydrous solvents saturated with nitrogen. Glass was heated under vacuum prior to use. Solvents were dried and distilled under nitrogen prior to use. The IR spectra were recorded with a Perkin-Elmer Spectrum 2000 FT-IR spectrometer as KBr pellets. NMR experiments (gHSQC, gHMBC, NOESY 1D, gCOSY) were recorded by using a Varian Mercury-VX 400 ($^1$H, 399.8; $^{13}$C, 100.6 MHz) or Unity Inova-600 ($^1$H, 600.0; $^{13}$C, 150.9 MHz). Abbreviations used are s (singlet), d (doublet), and m (multiplet). The spectra were referenced internally to residual solvent resonance. Electrospray mass spectra were recorded on a Waters ZQ-4000 spectrometer. Gas chromatography and GC-MS were performed on a HP6890 equipped with a 30 m × 0.2 mm Agilent DB-5 capillary column. General temperature program: 80 °C for 3 min, then 15 °C/min to 260 °C, which was maintained for 10 min. Crystal data were collected on a Bruker APEXII CCD diffractometer (Mo Kα radiation, $\lambda = 0.71073$ Å). An empirical absorption correction was applied, and the initial structure model was produced by direct methods. The structural solution was performed using the SHELXS-97 (Sheldrick, 1990) program, and structural refinement was performed using the SHELXL-97 (Sheldrick, 1997) program. The determination of the solubility was performed using a MLW T52.1 centrifuge. Cyclopentadiene (Aldrich, 98%) and cyclopentene oxide (Fluka, 98%) were used as received. Sodium cyclopentadienide (NaCp) was prepared as reported in the literature.[4d] Used abbreviations: $Cp^{OOO}H = C_5H_3[CH(CH)_3CHOH]_3$; $NaCp^{OOO} = C_5H_2[CH(CH)_3CHOH]_3Na$; nbd = 2,5-norbornadiene ($C_7H_8$); cod = 1,5-cyclooctadiene ($C_8H_{12}$); THF tetrahydrofurane; DME [$CH_3OCH_2CH_2OCH_3$]; $Et_2O$ diethyl ether; e.p. petroleum ether; GC-MS gas-chromatography–mass spectroscopy.

**Preparation of Sodium 1-(2-Hydroxycyclopentyl)cyclopenta-2,4-dien-1-ide, $NaCp^O$ (*rac*-1).** To a THF (20 mL) solution of sodium cyclopentadienide (1.00 g, 11.36 mmol) was added an equimolar amount of cyclopentene oxide (2.9 g, 11.4 mmol), and the mixture was then stirred for 12 h at room temperature. The solvent was then removed under vacuum, and the residue, after a fast filtration on a Celite pad, was washed with hexane (3 × 20 mL). Removal of volatiles afforded a purple powder as the title compound. Yield: 70% (1.38 g, 7.95 mmol).

**Quenching of *rac*-1 to $Cp^OH$: 2′-(Cyclopenta-1,3-dienyl)cyclopentanol, *rac*-1b, and 2′-(Cyclopenta-1,4-dienyl)cyclopentanol, *rac*-1c.** Solid *rac*-**1** (0.8 g, 4.6 mmol) was added to a saturated solution (20 mL) of $NaHCO_3$ in water. The aqueous phase was then extracted with diethyl ether (3 × 20 mL) and dried over $MgSO_4$. All volatile materials were removed under vacuum to leave a pasty yellow solid. Purification by column chromatography ($SiO_2$, 70–230 mesh, grade 60, 6:1 hexane/$Et_2O$) afforded the pure product as a pale yellow oil. Yield: 95% (0.74 g, 4.3 mmol).

*rac*-**1b**: Anal. Calcd for $C_{10}H_{14}O$: C, 79.94; H, 9.39. Found: C, 79.93; H, 9.38. ESI-MS (MeOH; *m*/*z* (%)): 190 (71) $[M + K]^+$, 173 (100) $[M + Na]^+$. $^1$H NMR (600 MHz, $CDCl_3$, $\delta$): 6.44, 6.10 (s, 3H, C*H*Cp), 4.10(m, 1H, C1′*H*OH), 2.97 (s, 2H$_5$, C$H_2$Cp), 2.76 (m, 1H, *C2′H*Cp), 2.03, 1.65 (m, 6H, C$H_2$ ring). $^{13}$C{$^1$H}NMR (150.9 MHz, $CDCl_3$, $\delta$): 145.16 (*ipso-C*), 136.10, 127.56, 124.12 (*C*HCp), 78.83 (*C*1′HOH), 49.72 (C2′HCp), 40.15 (*C*H$_2$Cp), 42.21, 34.20, 22.14 (*C*H$_2$ ring). IR (KBr, cm$^{-1}$): 3310.93 s ($\nu$OH), 2951.73 s ($\nu$CH$_2$), 1415.70, 1475.77 ($\nu$C=C).

*rac*-**1c**: Anal. Calcd for $C_{10}H_{14}O$: C, 79.94; H, 9.39. Found: C, 79.92; H, 9.39. ESI-MS (MeOH; *m*/*z* (%)): 190 (71) $[M + K]^+$, 173 (100) $[M + Na]^+$. $^1$H NMR (600 MHz, $CDCl_3$, $\delta$): 6.31, 6.26 (s, 3H, C*H*Cp), 4.05 (m, 1H, C1′*H*OH), 2.95 (s, 2H$_3$, C$H_2$Cp), 2.69 (m, 1H, C2′*H*Cp), 2.07, 1.58 (m, 6H, C$H_2$ ring). $^{13}$C{$^1$H}NMR (150.9 MHz, $CDCl_3$, $\delta$): 149.26 (*ipso-C*), 135.65, 129.12 126.72 (*C*HCp), 78.12 (*C*1′HOH), 45.39 (C2′HCp), 48.87 (*C*H$_2$Cp), 41.26, 34.13, 21.82 (*C*H$_2$ ring). IR (KBr, cm$^{-1}$): 3310.93 s ($\nu$OH), 2951.73 s ($\nu$CH$_2$), 1415.70, 1475.77 ($\nu$C=C).

**Preparation of Sodium 1,3-Bis(2-hydroxycyclopentyl)cyclopenta-2,4-dien-1-ide, $NaCp^{OO}$ (*rac*-2).** Sodium cyclopentadienide (1.00 g, 11.36 mmol) was dissolved in DME (20 mL). An excess of cyclopentene oxide (4.77 g, 22.8 mmol, 2 equiv) was then added, and the stirring mixture was refluxed for 10 h. The red-purple solution was dried under vacuum, affording a dark brown powder, which was washed with hexane, yielding the title compound as a brown powder. Yield: 75% (2.56 g, 8.52 mmol).

**Quenching of *rac*-2 to $Cp^{OO}H$: 2′,2″-(Cyclopenta-3,5-diene-1,3diyl)dicyclopentanol, *rac*-2c, and 2′,2″-(Cyclopenta-1,3-diene-1,3diyl)dicyclopentanol, *rac*-2d.** Solid *rac*-**2** (0.3 g, 1.16 mmol) was added to a saturated solution of $NaHCO_3$ in water (20 mL). The aqueous phase was then extracted with diethyl ether (3 × 20 mL) and dried over $MgSO_4$. All volatile materials were removed under vacuum. The product was obtained as an orange oil after fast filtration through a silica gel pad (70–230 mesh, grade 60) eluting with 1:1 hexanes/$Et_2O$. Yield: 75% (0.2 g, 0.87 mmol).

*rac*-**2c**: Anal. Calcd for $C_{15}H_{22}O_2$: C, 76.86; H, 9.46. Found: C, 76.85; H, 9.47. ESI-MS (MeOH; *m*/*z* (%)): 274 (32) $[M + K]^+$, 257 (100) $[M + Na]^+$. $^1$H NMR (600 MHz, $CDCl_3$, $\delta$): 6.07 (s, 2H, C*H*4,5Cp), 3.98 (m, 1H, C1′*H*OH+C1″*H*OH), 2.88 (s, 2H2, C$H_2$Cp), 2.70 (m, 1H, C2′*H*Cp + C2″*H*Cp), 2.23, 1.49 (m, 6H, C$H_2$ring). $^{13}$C{$^1$H}NMR (150.9 MHz, $CDCl_3$, $\delta$): 148.55, 148.25 (*ipso-C*), 127.72, 127.59 (*C*HCp), 79.06, 78.86 (*C*1′HOH + *C*1″HOH), 50.54, 50.28 (*C*2′HCp + *C*2′HCp), 45.68 (*C*H$_2$Cp), 41.47, 41.13, 34.14, 33.84, 29.76, 29.27 (*C*H$_2$ ring). IR (KBr, cm$^{-1}$): 3326.13 s ($\nu$OH), 2953.45 s ($\nu$CH$_2$), 1416.10, 1465.34 ($\nu$C=C).

*rac*-**2d**: Anal. Calcd for $C_{15}H_{22}O_2$: C, 76.86; H, 9.46. Found: C, 76.85; H, 9.47. ESI-MS (MeOH; *m*/*z* (%)): 274 (32) $[M + K]^+$, 257 (100) $[M + Na]^+$. $^1$H NMR (600 MHz, $CDCl_3$, $\delta$): 6.18, 5.89 (s, 2H, C*H*2,4Cp), 3.88 (m, 1H, C1′*H*OH +C1″*H*OH), 2.86 (s, 2H5, C$H_2$Cp), 2.73 (m, 1H, *C2′H*Cp + *C2″H*Cp), 2.13, 1.52 (m, 6H, C$H_2$ring). $^{13}$C{$^1$H}NMR (150.9 MHz, $CDCl_3$, $\delta$): 148.11, 147.94 (*ipso-C*), 126.83, 125.76 (*C*HCp), 78.83, 78.12 (*C*1′HOH + *C*1″HOH), 49.27, 47.72 (*C*2′HCp + *C*2′HCp), 45.59 (*C*H$_2$Cp), 41.42, 39.78, 33.92, 33.64, 29.72, 27.33 (*C*H$_2$ ring). IR (KBr, cm$^{-1}$): 3326.13 s ($\nu$OH), 2953.45 s ($\nu$CH$_2$), 1416.10, 1465.34 ($\nu$C=C).

**Preparation of Sodium 1,2,4-Tris(2-hydroxycyclopentyl)cyclopenta-2,4-dien-1-ide, $NaCp^{OOO}$ (*rac*-3).** To a DME (20 mL) solution of sodium cyclopentadienide (1.00 g, 11.36 mmol) was dissolved an excess of cyclopentene oxide (4.77 g, 56.8 mmol), and the stirring mixture was refluxed for 5 h. The obtained light brown precipitate was then filtered off and washed with petroleum ether. Yield: 94% (3.39 g, 10.67 mmol). The reaction is concluded when the $^1$H NMR spectrum of the anion, performed in Py-$d_5$ (Py = $C_5D_5N$), exhibits a broad resonance for the residual C*H*Cp protons at $\delta$ 4.65–4.30 and a characteristic broad signal centered at $\delta$ 6.20 for the overlapped OH groups.

**Quenching of *rac*-3 to $Cp^{OOO}H$: 2′,2″,2‴-(Cyclopenta-1,3-diene-1,2,4-tryil)tricyclopentanol, *rac*-3b, and 2′,2″,2‴-(Cyclopenta-1,4-diene-1,2,4-tryil)tricyclopentanol, *rac*-3c.** To a saturated solution of $NaHCO_3$ in water (20 mL) was added solid *rac*-**3** (0.5 g, 1.46 mmol). The aqueous phase was then extracted with diethyl ether (3 × 20 mL) and dried over $MgSO_4$. After column chromatography in $SiO_2$ (70–230 mesh, grade 60) by eluting with $Et_2O$ and solvent removal, an orange microcrystalline powder was obtained. Yield: 70% (0.32 g, 1.02 mmol). Two-dimensional NMR experiments, performed on the neutral cyclopentadiene derivative $Cp^{OOO}H$, confirm the 1,2,4 position for the tethered alcohol substituents. The stereochemistry has been attributed by 1D NOESY experiments.

*rac*-**3b**: Anal. Calcd for $C_{20}H_{30}O_3$: C, 75.41; H, 9.50. Found: C, 75.42; H, 9.49. ESI-MS (MeOH; *m*/*z* (%)): 357 (74) $[M + K]^+$,

341 (100) $[M + Na]^+$, 336 (100) $[M + NH_4]^+$. $^1H$ NMR (600 MHz, $CDCl_3$, $\delta$): 6.10 (s, 1H, C*H*3Cp), 4.56 (m, br, 3O*H*), 3.92 (m, 2H, C1′*H*OH + C1″*H*OH), 3.80 (m, 1H, C1‴*H*OH), 2.9 (s, 2H, C$H_2$Cp), 2.85 (m, 1H, *C*2′*H*Cp + *C*2″*H*Cp), 2.78 (m, 1H, *C*2‴*H*Cp), 2.02, 1.74, 1.68, 1.56 (m, 27H, C$H_2$ring). $^{13}C\{^1H\}$NMR (150.9 MHz, $CDCl_3$, $\delta$): 148.66, 142.56, 141.01 (*ipso-C*), 126.21 (*C*3), 79.33 (*C*1′HOH + *C*1″HOH), 78.49 (*C*1‴HOH), 46.15 (*C*2‴HCp), 47.49 (*C*2′HCp), 50.79 (*C*2″HCp), 41.55 (*C*$H_2$), 37.12, 35.81, 34.23, 29.64, 22.32, 21.15 (*C*$H_2$ ring). IR (KBr, $cm^{-1}$): 3380.73 s, sh ($\nu$OH), 2952.03 s ($\nu CH_2$), 1450.70, 1455.17 ($\nu$C═C).

*rac*-**3c**: Anal. Calcd for $C_{20}H_{30}O_3$: C, 75.41; H, 9.50. Found: C, 75.42; H, 9.49. ESI-MS (MeOH; *m*/*z* (%)): 357 (74) $[M + K]^+$, 341 (100) $[M + Na]^+$, 336 (100) $[M + NH_4]^+$. $^1H$ NMR (600 MHz, $CDCl_3$, $\delta$): 6.10 (s, 1H, C*H*3Cp), 3.90 (m, 2H, C1′*H*OH + C1″*H*OH), 3.78 (m, 1H, C1‴*H*OH), 2.88 (s, 2H, C$H_2$Cp), 2.86 (m, 1H, *C*2′*H*Cp + *C*2″*H*Cp), 2.76 (m, 1H, *C*2‴*H*Cp) 2.01, 1.76, 1.64, 1.57 (m, 27H, C$H_2$ ring). $^{13}C\{^1H\}$ NMR (150.9 MHz, $CDCl_3$, $\delta$): 148.33, 142.46, 141.02 (*ipso-C*), 127.36 (s, *C*5), 79.44 (*C*1′HOH + *C*1″HOH), 78.39 (*C*1‴HOH), 46.78 (*C*2‴HCp), 47.15 (*C*2′HCp), 51.11 (*C*2″HCp), 40.03 (*C*$H_2$), 37.87, 36.11, 34.56, 28.14, 23.12, 22.45 (*C*$H_2$ ring). IR (KBr, $cm^{-1}$): 3380.73 s, sh ($\nu$OH), 2952.03 s ($\nu CH_2$), 1450.70, 1455.17 ($\nu$C═C).

**Preparation of $Cp^{OOO}$Rh(nbd) (*rac*-4). (a) Thermal Procedure.** To a stirred THF (40 mL) solution of *rac*-**3** $Cp^{OOO}Na$ (0.72 g, 2.12 mmol) was added $[Rh(nbd)Cl]_2$ (0.48 g, 1.06 mmol, 0.5 equiv) in the same solvent. The refluxed solution after 5 h darkened to deep brown. After solvent removal the black powder was washed several times with $Et_2O$ (3 × 30 mL). Under vacuum the filtered solution yielded crude *rac*-**4** as an ochre microcrystalline solid. Yield: 94% (1.02 g, 1.99 mmol). The silica column chromatography (70–230 mesh, grade 60) with $Et_2O$/THF (1:1) as eluent gives rise to two distinct dark yellow fractions, affording *rac*-**4a** (I, 73.5%) and *rac*-**4c** (II, 20.5%).

**(b) Room-Temperature Procedure.** The reaction was stirred in THF for 37 h at room temperature, by utilizing the same amount. Separation of the crude *rac*-**4** was performed on silica TLC preparative plates (20 × 20 cm, polyester, grade 60) with $Et_2O$/THF (1:1) as eluting solution. Two distinct dark yellow fractions were obtained and identified as *rac*-**4a** (I, 70.5%) and *rac*-**4b** + *rac*-**4c** (II, 23.5%). Yield: 94%.

*rac*-**4a**: Anal. Calcd for $C_{27}H_{37}O_3Rh$: C, 63.25; H, 7.28. Found: C, 63.24; H, 7.29. ESI-MS (MeOH; *m*/*z* (%)): 535 (100) $[M + Na]^+$, 512 (9.7) $[M + H]^+$, 341 (28) $[(M - Rh(nbd)) + Na]^+$. $^1H$ NMR (600 MHz, $CDCl_3$, $\delta$): 4.93 (d, 1H, $J_{Rh\text{-}H} = 1.2$ Hz, C*H*3Cp), 4.85 (d, 1H, $J_{Rh\text{-}H} = 1.2$ Hz, C*H*5Cp), 3.93 (m, 1H, C1‴*H*OH), 3.78 (m, 2H, C1′*H*OH + C1″OH), 3.38 (m, 2H, C5,6*H*, nbd), 3.17 (m; br, 4H, C1,2,3,4*H*, nbd), 2.44 (m, 3H, *C*2′*H*Cp + *C*2″*H*Cp + *C*2‴*H*Cp), 2.01 (m, 6H, C$H_2$ ring), 1.64 (m, 12H, C$H_2$ ring), 1.00 (s, 2H, C$H_2$-nbd), 3.88, 3.36, 2.94 (s, 3H, O*H*). $^{13}C\{^1H\}$ NMR (150.9 MHz, $CDCl_3$, $\delta$): 106.11, 105.56, 105.40 (d, *ipso-C*, $J_{Rh\text{-}C}$ = 19 Hz), 80.71 (d, *C*H3-Cp, $J_{Rh\text{-}C} = 4$ Hz), 80.38 (d, *C*H5-Cp, $J_{Rh\text{-}C} = 4$ Hz), 79.72, 78.83, 78.77 (*C*1′HOH + *C*1″HOH + *C*1‴HOH), 58.30 (d, *C*$H_2$-nbd, $J_{Rh\text{-}C} = 6.4$), 47.17, 47.15 (*C*5,6H-nbd), 47.63, 45.65, 45.52 (*C*2′HCp + *C*2″HCp + *C*2‴HCp), 31.93, 31.88, 31.65, 31.55 (d, *C*1,2,3,4H, nbd, $J_{Rh\text{-}C} = 10.5$ Hz), 34.54, 34.37, 34.28, 33.79, 32.54, 22.08, 21.54, 21.43 (*C*$H_2$ ring).

*rac*-**4c**: Anal. Calcd for $C_{27}H_{37}O_3Rh$: C, 63.25; H, 7.28. Found: C, 63.23; H, 7.26. ESI-MS (MeOH; *m*/*z* (%)): 535 (100) $[M + Na]^+$, 512 (28) $[M + H]^+$, 341 (26) $[(M - Rh(nbd)) + Na]^{+\cdot}$ $^1H$ NMR (600 MHz, $CDCl_3$, $\delta$): 4.92 (d, 1H, $J_{Rh\text{-}H} = 1.2$ Hz, C*H*3Cp), 4.75 (d, 1H, $J_{Rh\text{-}H} = 1.2$ Hz, C*H*5Cp), 3.38 (s, 2H, O*H*, 1,2), 3.20 (s, 1H, O*H*, 4), 3.85 (m, 3H, C1′*H*OH + C1-*H*OH + C1′-*H*OH), 3.30 (m, 2H, C5,6*H*, nbd), 3.73 (d, 2H, C1,2*H*, nbd), 3.37 (d, 2H, C3,4*H*, nbd), 2.35 (m, 1H, *C*2′*H*Cp), 2.75 (m, 1H, *C*2″*H*Cp), 2.85 (m, 1H, *C*2‴*H*Cp), 2.04 (m, 9H, C$H_2$ ring), 1.64 (m, 9H, C$H_2$ ring), 0.92 (m, 2H, C$H_2$-nbd). $^{13}C\{^1H\}$NMR (150.9 MHz, $CDCl_3$, $\delta$): 107.09, 106.44, 106.09 (d, *ipso-C*, $J_{Rh\text{-}C} = 19$ Hz), 81.20 (d, *C*H3Cp, $J_{Rh\text{-}C} = 4$ Hz), 79.27 (d, *C*H5Cp, $J_{Rh\text{-}C} = 4$ Hz), 82.15, 82.03, 79.17 (*C*1′HOH + *C*1″HOH + *C*1‴HOH), 47.84 (*C*2′HCp), 46.04 (*C*2″HCp), 45.91 (*C*2‴HCp), 47.13, 47.11 (*C*5,6H, nbd), 30.85, 30.74, 30.60, 30.51 (d, *C*1,2,3,4H, nbd, $J_{Rh\text{-}C} = 10$ Hz), 57.85 (d, *C*$H_2$, nbd, $J_{Rh\text{-}C} = 18$ Hz), 36.05, 35.93, 34.66, 33.47, 33.11, 23.12, 20.84 (*C*$H_2$ ring).

*rac*-**4b**: Anal. Calcd for $C_{27}H_{37}O_3Rh$: C, 63.25; H, 7.28. Found: C, 63.25; H, 7.27. ESI-MS (MeOH; *m*/*z* (%)): 535 (100) $[M + Na]^+$, 512 (28) $[M + H]^+$, 341 (26) $[(M - Rh(nbd)) + Na]^+$. $^1H$ NMR (600 MHz, $CDCl_3$, $\delta$): 4.91 (d, 1H, $J_{Rh\text{-}H} = 1.2$ Hz, C*H*3Cp), 4.73 (d, 1H, $J_{Rh\text{-}H} = 1.2$ Hz, C*H*5Cp), 3.85 (m, 3H, C1′*H*OH + C1″*H*OH + C1‴*H*OH), 2.48 (m, 2H, *C*2′*H*Cp + *C*2″*H*Cp), 2.25 (m, *C*2‴*H*Cp).

**Preparation of $Cp^{OOO}$Rh(cod) (*rac*-5).** To a THF (30 mL) solution of *rac*-**3**, $Cp^{OOO}Na$ (0.72 g, 2.12 mmol), was added $[Rh(cod)Cl]_2$ (0.52 g, 1.06 mmol, 0.5 equiv) in the same solvent. The refluxing solution after 5 h darkened to deep red. The powder obtained after solvent removal was washed several times with $Et_2O$ (3 × 30 mL) and filtered in a Celite pad (2 cm). The filtered solution yielded under vacuum the crude *rac*-**5** as a red microcrystalline mixture of the two diastereoisomers *rac*-**5a** and *rac*-**5c**. Yield: 93% (1.04 g, 1.97 mmol). The separation by silica column chromatography (70–230 mesh, grade 60) with $Et_2O$/THF (1:2) as eluent gives rise to two distinct dark red fractions, affording *rac*-**5a** (I, 73.5%) and *rac*-**5c** (II, 19.5%).

*rac*-**5a**: Anal. Calcd for $C_{28}H_{41}O_3Rh$: C, 63.61; H, 7.82. Found: C, 63.62; H, 7.82. ESI-MS (MeOH; *m*/*z* (%)): 551 (100) $[M + Na]^+$, 528 (35) $[M + H]^+$, 341 (28) $[(M - Rh(cod)) + Na]^+$. $^1H$ NMR (400 MHz, $CDCl_3$, $\delta$): 4.93 (d, 1H, $J_{Rh\text{-}H} = 1.8$ Hz, C*H*3Cp), 4.81 (d, 1H, $J_{Rh\text{-}H} = 1.8$ Hz, C*H*5Cp), 3.87 (m, 1H, C1‴*H*OH), 3.82 (m, 2H, C1′*H*OH + C1″*H*OH), 3.36 (m, 4H, C*H*, cod), 2.72 (m, 3H, *C*2′*H*Cp+ *C*2″*H*Cp + *C*2‴*H*Cp), 2.21 (m, 6H, C$H_2$ ring), 1.72 (m, 12H, C$H_2$ ring), 2.04, 1.43 (m, 8H, C$H_2$-cod). $^{13}C\{^1H\}$ NMR (100.59 MHz, $CDCl_3$, $\delta$): 107.16, 106.29, 105.10 (d, *ipso-C*, $J_{Rh\text{-}C} = 22$ Hz), 79.91 (d, *C*H3Cp, $J_{Rh\text{-}C} = 4$ Hz), 79.18 (d, *C*H5Cp, $J_{Rh\text{-}C} = 4$ Hz), 78.12, 77.93, 77.67 (*C*1′HOH + *C*1″HOH + *C*1‴HOH), 46.15, 45.85 (*C*H-cod), 47.36, 46.15, 45.62 (*C*2′HCp + *C*2″HCp + *C*2‴HCp), 34.14, 33.77, 32.12, 22.08, 21.74, 21.03 (*C*$H_2$ ring), 33.19, 32.54, 31.16, 30.03 (*C*$H_2$-cod).

*rac*-**5c**: Anal. Calcd for $C_{28}H_{41}O_3Rh$: C, 63.61; H, 7.82. Found: C, 63.61; H, 7.83. ESI-MS (MeOH; *m*/*z* (%)): 551 (100) $[M + Na]^+$, 528 (28) $[M + H]^+$, 341 (26) $[(M - Rh(cod)) + Na]^+$. $^1H$ NMR (400 MHz, $CDCl_3$, $\delta$): 5.04 (d, 1H, $J_{Rh\text{-}H} = 1.8$ Hz, C*H*3Cp), 4.94 (d, 1H, $J_{Rh\text{-}H} = 1.8$ Hz, C*H*5Cp), 3.91 (m, 1H, C1‴*H*OH), 3.79 (m, 2H, C1′*H*OH + C1″*H*OH), 3.41 (m, 4H, C*H*, cod), 2.67 (m, 3H, *C*2′*H*Cp + *C*2″*H*Cp + *C*2‴*H*Cp), 2.31 (m, 6H, C$H_2$ ring), 1.76 (m, 12H, C$H_2$ ring), 2.10, 1.503 (m, 8H, C$H_2$-cod). $^{13}C\{^1H\}$ NMR (100.59 MHz, $CDCl_3$, $\delta$): 108.21, 107.79, 106.56 (d, *ipso-C*, $J_{Rh\text{-}C} = 22$ Hz), 80.71 (d, *C*H3Cp, $J_{Rh\text{-}C} = 4$ Hz), 79.98 (d, *C*H5Cp, $J_{Rh\text{-}C} = 4$ Hz), 78.86, 78.33, 77.47 (*C*1′HOH + *C*1″HOH + *C*1‴HOH), 46.55, 44.25 (*C*H-cod), 47.06, 45.75, 45.12 (*C*2′HCp + *C*2″HCp + *C*2‴HCp), 33.54, 33.11, 32.62, 22.43, 21.15, 20.93 (*C*$H_2$ ring), 34.29, 33.764, 31.22, 30.34 (*C*$H_2$-cod).

**Preparation of $Cp^{OOO}Rh(C_2H_4)_2$ (*rac*-6).** To a Schlenk flask charged with *rac*-**3**, $Cp^{OOO}Na$ (0.34 g, 1.00 mmol), was added THF (25 mL) under argon. The resulting solution was stirred at room temperature, and $[Rh(C_2H_4)_2Cl]_2$ (0.23 g, 0.5 mmol, 0.5 equiv) was added. The clear solution was stirred for 4 h at reflux, and the color changed from brown to dark red. After the solvent was removed under vacuum, 50 mL of $Et_2O$ was added. The solution was filtered through a Celite pad (2 cm), giving a dark red solution. The separation by alumina chromatography (8% water deactivated) with $Et_2O$/THF (1:1) as eluent gives rise to two distinct deep red fractions, affording *rac*-**6a** (I, 70.5%) and *rac*-**6c** (II, 16.5%). Yield: 87%.

*rac*-**6a**: Anal. Calcd for $C_{24}H_{37}O_3Rh$: C, 60.48; H, 7.83. Found: C, 60.48; H, 7.82. ESI-MS (MeOH; *m*/*z* (%)): 498 (100) [M +

Na]$^+$, 475 (16) [M + H]$^+$, 341 (36) [(M − Rh($C_2H_4$)$_2$) + Na]$^+$. $^1$H NMR (600 MHz, $CDCl_3$, $\delta$): 4.89 (s, 1H, C*H*3Cp), 4.47 (s, 1H, C*H*5Cp), 4.12 (s, br, 3H, O*H*), 3.78 (m, 2H, C1′*H*OH + C1″*H*OH), 3.93 (m, 1H, C1‴*H*OH), 2.45 (m, 2H, *C2′H*Cp + *C2″H*Cp), 2.32 (m, 1H, *C2‴H*Cp), 2.80 (s, br, 4H, C$H_2$-$C_2H_4$), 1.34 (m, 4H, C$H_2$-$C_2H_4$), 1.95 (m, br, 6H, C$H_2$ ring), 1.61 (m, br, C$H_2$ ring). $^{13}$C{$^1$H} NMR (150.9 MHz, $CDCl_3$, $\delta$): 108.41, 107.93, 106.13 (d, *ipso-C*-Cp, $J_{Rh\text{-}C}$ = 14 Hz), 83.24 (d, *C*H3Cp, $J_{Rh\text{-}C}$ = 4 Hz), 83.20 (d, *C*H5Cp, $J_{Rh\text{-}C}$ = 4 Hz), 78.63, 77.28 (*C1′*HOH + *C1″*HOH), 76.96 (*C1‴*HOH), 46.88 (*C2‴*HCp), 46.67, 45.11 (*C2′*HCp + *C2″*HCp), 34.81, 34.48, 34.31, 34.09, 32.00, 21.88, 21.29, 21.23 (*C*H$_2$ ring), 40.98, 40.82, 40.75, 40.02 (*C*H$_2$-$C_2H_4$).

*rac*-**6c**: Anal. Calcd for $C_{24}H_{37}O_3Rh$: C, 60.48; H, 7.83. Found: C, 60.46; H, 7.83. ESI-MS (MeOH, *m*/*z* (%)): 498 [M + Na]$^+$ (100), 475 [M + H]$^+$ (12), 341 (6) [(M − Rh($C_2H_4$)$_2$) + Na]$^+$. $^1$H NMR (600 MHz, $CDCl_3$, $\delta$): 4.93 (s, 1H, C*H*3Cp), 4.65 (s, 1H, C*H*5Cp), 3.22 (s, br, 3H, O*H*), 3.76 (m, 2H, C1′*H*OH + C1″*H*OH), 3.90 (m, 1H, C1‴*H*OH), 2.69 (m, 2H, *C2′H*Cp + *C2″H*Cp), 2.23 (m, 1H, *C2‴H*Cp), 2.78 (s, br, 4H, C$H_2$-$C_2H_4$), 1.24 (m, 4H, C$H_2$-$C_2H_4$), 1.97 (m, br, 6H, C$H_2$ ring), 1.68 (m, br, C$H_2$ ring). $^{13}$C{$^1$H} NMR (150.9 MHz, $CDCl_3$, $\delta$): 106.81, 106.03, 105.61 (d, *ipso-C*-Cp, $J_{Rh\text{-}C}$ = 14 Hz), 82.76 (d, *C*H3Cp, $J_{Rh\text{-}C}$ = 4 Hz), 81.80 (d, *C*H5Cp, $J_{Rh\text{-}C}$ = 4 Hz), 81.62, 79.12 (*C1′*HOH + *C1″*HOH), 78.82 (*C1‴*HOH), 45.67 (*C2‴*HCp), 45.11, 44.63 (*C2′*HCp + *C2″*HCp), 35.11, 34.78, 34.01, 33.49, 32.40, 21.08, 20.72, 20.13 (*C*H$_2$ ring), 40.18, 39.93, 38.75, 41.56 (*C*H$_2$-$C_2H_4$).

**Preparation of Cp$^{OOO}$Rh(CO)$_2$ (*rac*-7).** To a stirred solution of *rac*-**3**, Cp$^{OOO}$Na (0.52 g, 1.52 mmol), in THF (20 mL) was added [Rh(CO)$_2$Cl]$_2$ (0.3 g, 0.76 mmol, 0.5 equiv), and the resulting solution was refluxed for 12 h. The reaction was monitored by IR in solution (THF). After cooling, the gray powder obtained after solvent removal was washed several times with dry $Et_2O$ (4 × 30 mL) and filtered over a Celite pad (3 cm), giving a dark blue solution. The filtered solution yielded under vacuum the crude *rac*-**7** as a blue microcrystalline mixture of the two diastereoisomers *rac*-**7a** and *rac*-**7c**. Yield: 96% (1.04 g, 1.97 mmol). Separation by silica column chromatography (70–230 mesh, grade 60) with THF as eluent gives rise to two distinct fractions, affording *rac*-**7a** (I, 73.5%) and *rac*-**7c** (II, 22.5%).

*rac*-**7a**: Anal. Calcd for $C_{22}H_{29}O_5Rh$: C, 55.44; H, 6.13. Found: C, 55.44; H, 6.12. ESI-MS (MeOH; *m*/*z* (%)): 499 (100) [M + Na]$^+$, 476 (8) [M + H]$^+$, 341 (56) [(M − Rh(CO)$_2$) + Na]$^+$. IR ($\nu$, cm$^{-1}$): 2025, 1959 ($\nu_{CO}$). $^1$H NMR (600 MHz, $CDCl_3$, $\delta$): 5.20 (s, 1H, C*H*$_3$-Cp), 5.11 (s, 1H, C*H*5Cp), 4.47 (s, br, 2H, O*H*), 3.87 (m, 2H, C1′*H*OH + C1″*H*OH), 3.61 (m, 1H, C1‴*H*OH), 3.13 (s, br, 1H, O*H*(4)), 2.75 (m, 2H, *C2′H*Cp + *C2″H*Cp), 2.32 (m, 1H, *C2‴H*Cp), 2.05 (m, br, 6H, C$H_2$ ring), 1.67 (m, br, C$H_2$ ring). $^{13}$C{$^1$H} NMR (150.9 MHz, $CDCl_3$, $\delta$): 192.66 (d, *C*O, $J_{Rh\text{-}C}$ = 82 Hz), 112.69, 112.26, 112.04 (d, *ipso-C*, $J_{Rh\text{-}C}$ = 14 Hz), 82.84 (d, *C*H3Cp, $J_{Rh\text{-}C}$ = 4 Hz); 81.40 (d, *C*H5Cp, $J_{Rh\text{-}C}$ = 4 Hz), 80.16, 79.96 (*C1′*HOH + *C1″*HOH), 78.35 (*C1‴*HOH), 46.68 (*C2‴*HCp); 44.69, 44.65 (*C2′*HCp + *C2″*HCp), 36.30, 35.84, 35.81, 33.41, 33.18, 22.21, 22.16, 20.36 (*C*H$_2$ ring).

*rac*-**7c**: Anal. Calcd for $C_{22}H_{29}O_5Rh$: C, 55.44; H, 6.13. Found: C, 55.43; H, 6.13. ESI-MS (MeOH, *m*/*z* (%)): 499 [M + Na]$^+$ (100), 476 [M + H]$^+$ (8), 341 (36) [(M − Rh(CO)$_2$)+Na]$^+$. IR ($\nu$, cm$^{-1}$): 2027, 1961 ($\nu_{CO}$). $^1$H NMR (600 MHz, $CDCl_3$, $\delta$): 5.26 (s, 1H, C*H*3Cp), 5.21 (s, 1H, C*H*5Cp), 4.19 (s, br, 2H, O*H*), 3.56 (m, 2H, C1′*H*OH + C1″*H*OH), 3.46 (m, 1H, C1‴*H*OH), 3.19 (s, br, 1H, O*H*), 2.48 (m, 3H, *C2′H*Cp + *C2″H*Cp + *C2‴H*Cp), 2.09 (m, br, 9H, C$H_2$ ring), 1.68 (m, br, 9H, C$H_2$ ring). $^{13}$C{$^1$H} NMR (150.9 MHz, $CDCl_3$, $\delta$): 192.11 (d, *C*O, $J_{Rh\text{-}C}$ = 82 Hz), 113.04, 112.93, 112.52 (d, *ipso-C*, $J_{Rh\text{-}C}$ = 14 Hz), 83.95 (d, *C*H3Cp, $J_{Rh\text{-}C}$ = 4 Hz), 82.58 (d, *C*H5Cp, $J_{Rh\text{-}C}$ = 4 Hz), 80.73, 80.49 (*C1′*HOH + *C1″*HOH), 79.88 (*C1‴*HOH), 46.50, 45.08, 44.84 (*C2′*HCp + *C2″*HCp+ *C2‴*HCp), 35.87, 34.03, 33.71, 33.56, 33.13, 33.09, 32.86, 22.71, 21.20, 21.06, 20.72, 20.38 (*C*H$_2$ ring).

**Table 4. Summary of Crystallographic Data and Structure Refinement Details for *rac*-4a**

| chem formula | $C_{27}H_{37}O_3Rh \cdot CHCl_3$ |
|---|---|
| fw | 631.84 |
| *T*, K | 100(2) |
| cryst size, mm | 0.20 × 0.25 × 0.30 |
| cryst syst | triclinic |
| space group | $P\bar{1}$ |
| *a*, Å | 9.6097(4) |
| *b*, Å | 11.3454(5) |
| *c*, Å | 14.8142(7) |
| α, deg | 104.724(1) |
| *β*, deg | 96.667(1) |
| *γ*, deg | 115.065(1) |
| *V*, Å$^3$ | 1368.05(11) |
| *Z* | 2 |
| $D_{calcd}$, g cm$^{-3}$ | 1.534 |
| $\mu$, mm$^{-1}$ | 0.945 |
| *F*(000) | 652 |
| $\theta$ range, deg | 1.47−28.69 |
| no. of measd reflns | 12 021 |
| no. of unique reflns | 5849 ($R_{int}$ = 0.0144) |
| goodness-of-fit | 1.057 |
| final *R* indices [$I > 2\sigma(I)$] | R1($F$)$^a$ = 0.0399, wR2($F^2$)$^b$ = 0.0988 |
| largest diff peak and hole, e Å$^{-3}$ | 0.107 and −1.799 |

$^a$ R1 = $\sum||F_o|-|F_c|/\sum|F_o|$. $^b$ wR2 = $[\sum w(F_o^2 - F_c^2)^2/\sum w(F_o^2)^2]^{1/2}$ where $w = 1/[\sigma^2(F_o^2) + (aP)^2 + bP]$ where $P = (F_o^2 + 2F_c^2)/3$.

**X-ray Crystal Structure Determination of *rac*-4a.** Single crystals of complex *rac*-**4a** were obtained by slow vapor diffusion of pentane into a $CDCl_3$ solution of *rac*-**4a** at −18 °C. X-ray diffraction intensities for *rac*-**4a** were collected on a Bruker SMART APEX II CCD diffractometer (Mo Kα radiation, $\lambda$ 0.71073 Å) at 100 K. Cell dimensions and the orientation matrix were initially determined from a least-squares refinement on reflections measured in three sets of 20 exposures, collected in three different $\omega$ regions, and eventually refined against all data. A full sphere of reciprocal space was scanned by 0.3° $\omega$ steps. The software SMART[13] was used for collecting frames of data, indexing reflections, and determining lattice parameters. The collected frames were then processed for integration by the SAINT program,[14] and an empirical absorption correction was applied using SADABS.[13]The structure was solved by direct methods (SIR 97)[15] and subsequent Fourier syntheses and refined by full-matrix least-squares on $F^2$ (SHELXTL),[16] using anisotropic thermal parameters for all non-hydrogen atoms. All hydrogen atoms were located in the Fourier map and, except the methyne hydrogens, which were refined isotropically, added in calculated positions, included in the final stage of refinement with isotropic thermal parameters $U$(H) = 1.2$U$($C_{Cp}$) and $U$(H) = 1.3$U$(C), and allowed to ride on their carrier carbons. Crystal data and details of data collection for *rac*-**4a** are reported in Table 4.

**Determination of the Partition Coefficient octanol/water ($K_{ow}$).** The $K_{ow}$ was determined with the described shake-flask procedure:[5b] 100 mg (0.19 mmol) of *rac*-**4a** was introduced into a separating funnel with the two phases (10 mL of *n*-octanol and 10 mL of water) and shaken for a period long enough for the equilibrium to be achieved (10 min). The concentration of the rhodium complex in each phase (g L$^{-1}$, $C_o$ 80%; $C_w$ 68.7%) is determined after phase separation and solvent removal: log $K_{ow}$ = −0.071.

(13) *SMART* & *SAINT* Software Reference Manuals, version 5.051 (Windows NT Version); Bruker Analytical X-ray Instruments Inc.: Madison, WI, 1998.

(14) Sheldrick, G. M. *SADABS, program for empirical absorption correction*; University of Göttingen: Germany, 1996.

(15) Altomare, A.; Cascarano, G.; Giacovazzo, C.; Guagliardi, A.; Moliterni, A. G. G.; Burla, M. C.; Polidori, G.; Camalli, M.; Siliqi, D. *Acta Crystallogr., Sect. A* **1996**, *52*, C79.

(16) Sheldrick, G. M. *SHELXTL plus (Windows NT Version) Structure Determination Package*, Version 5.1; Bruker Analytical X-ray Instruments Inc.: Madison, WI, 1998.

**Determination of Solubility in Water ($S_w$) or Benzene ($S_b$).** Solubility in water and in benzene has been established by measuring the solubility coefficient at room temperature, $S_w$ = 15.9 g $L^{-1}$ and $S_b$ = 8.6 g $L^{-1}$.[5c] The rhodium complex *rac*-**4a** and the solvent (1 mL) were introduced into a microcentrifuge tube (1.5 mL) and then stirred for 1 h in a centrifuge at low rate (2 rpm). In order to separate the solid phase from the liquid phase, the microcentrifuge tube was then stirred at high rate (9 rpm) for 20 min. The $Cp^{OOO}Rh(nbd)$, *rac*-**4a**, complex (100 mg, 0.19 mmol) was left to stir for 12 h in EtOH/$H_2O$ (1:1) solution. Uncorrupted compound (85%) was then recovered and its nature confirmed by $^1H$ NMR.

**Determination of the Air Stability of *rac*-4.** (a) Solid: the air stability of the rhodium complex $Cp^{OOO}Rh(nbd)$, *rac*-**4a**,**c**, has been evaluated; ca. 70 mg (0.137 mmol) of pure *rac*-**4a** was exposed to air for one week. The residue dissolved in THF solution and filtrated under a $SiO_2$ pad was then examined by $^1H$ NMR spectrum in the Cp range, confirming the nature of the title compound.

(b) Solution: 70 mg of pure *rac*-**4a** was left to stir in a chloroform solution for 10 days. The $^1H$ NMR spectrum in $CDCl_3$ confirms the exclusive presence of pure *rac*-**4a**.

**$^1H$ NMR Experiments of *rac*-4a and *rac*-4c with Chiral Solvating Agents (Pirkle's alcohol).** The addition of shift reagent 1-anthracen-9-yl-2,2,2-trifluoroethanol [Pirkle's alcohol][7] to a benzene-$d_6$ solution of crystalline **4a** confirms the 1:1 splitting of the C*H*Cp signals, typical of racemic compounds. $^1H$ NMR (600 MHz, $CDCl_3$, 25 °C, TMS): *rac*-**4a** [+Pirkle] 4.67, 4.65 (s, 1*H*3), 4.42, 4.39 (s, 1*H*5); *rac*-**4c** [+Pirkle] 4.58, 4.56 (s, 1*H*3), 4.37, 4.35 (s, 1*H*5).

**Computational Details.** Ab initio DFT calculations have been performed using the ADF 2005 quantum chemistry package,[17] using the built-in TZP basis and the BLYP functional.[18] Inner orbitals (1s for carbon and oxygen and 3d for rhodium) have been kept frozen; this corresponds to the "small core" option in the definition of the basis set for the ADF code. Geometry optimizations were carried out in Cartesian coordinates using convergence criteria slightly tighter than default ($10^{-5}$ for energies and $10^{-3}$ for gradients).

**Acknowledgment.** We thank the University of Bologna and the MIUR for supporting this work and Prof. Paolo Biscarini (University of Bologna) for helpful discussions.

**Supporting Information Available:** $^1H$ NMR/$^{13}C$ NMR spectra of *rac*-**3b**,**c** (Figure S1 and S2). $^1H$ NMR/$^{13}C$ NMR/HSQC spectra of *rac*-**4a**,**c** (Figures S3, S4, S5, S6, S7, and S8). NOESY contacts for the *rac*-**4a** and *rac*-**4c** rhodium complexes (Figures S9 and S10). The crystallographic data are also given as CIF files. This material is available free of charge via the Internet at http://pubs.acs.org. X-ray data have also been deposited at the CCDC, Cambridge U.K., under deposit number 654075.

OM701073H

(17) Te Velde, G. ; Bickelhaupt, F. M.; Baerends, E. J.; Fonseca Guerra, C.; Van Gisbergen, S. J. A.; Snijders, J. G.; Ziegler, T. *J. Comput. Chem.* **2001**, *22*, 931–967.

(18) (a) Becke, A. D. *Phys. Rev. A* **1988**, *38*, 3098–3100. (b) Lee, T.; Yang, W. T.; Parr, R. G. *Phys. Rev. B.* **1988**, *37*, 785–789.